Conductive inks printing through laser-induced forward transfer

Author: Pol Sopeña i Martínez
Departament de Física Aplicada i Òptica,
Facultat de Física, Universitat de Barcelona,
Martí i Franquès 1, 08028 Barcelona, Spain.

Advisor: Pere Serra Coromina

Abstract: The laser-induced forward transfer of silver nanoparticle ink with long laser pulse duration (120 *ns*) was investigated in this work. The feasibility of the technique for printing patterns was proven. The study focuses on the analysis of the deposition of droplets and transfer dynamics. Several droplets were printed at different laser pulse energies, showing a radius-energy linear dependence. However, the volume-energy dependence was non-monotonous, increasing at low energies and staying fairly constant at high ones. A time-resolved study of the transfer dynamics showed four stages during the transfer process: bubble expansion, bubble burst, jet formation and deposition, which always occur independently of the energy. A feasibility test was also carried out to prove the functionality of printed lines as interconnects in electronic circuits.

I. INTRODUCTION

Material transfer techniques appear from the necessity to transfer those materials from one source to a substrate without altering their properties. Many techniques are available, yet the two main ones are nozzle based techniques, like inkjet printing [1], and laser-direct write (LDW+) addition processes [2]. Both techniques have the ability to transfer liquid materials, with some limitations though. Inkjet printing is much more accessible and has been explored till turning it into a commercial technique. However, there are some restrictions concerning liquid viscosity requirements, nozzle clogging or head contamination issues. On the other side, LDW+ techniques are not so widespread but they do not present many limitations in viscosities, and since there is no nozzle the material can be transferred without clogging problems.

From all the possible LDW+ techniques Laser-Induced Forward Transfer (LIFT) is the most extended approach to transfer inks and solutions [3]. The technique has been widely studied [2–4] and its feasibility has been demonstrated even with the realization of an industrial-scale device [5]. Transferred materials range from inorganic materials like conductive inks [6], to organic materials such polymers [7] or bio-samples such as DNA for biosensors [8].

The underlying principle of the technique consists on using a laser pulse to propel material from a donor film to an acceptor substrate. As shown in Fig.1 the donor substrate is covered with a film of the material to transfer, liquid in this case, and separated a convenient gap distance from the acceptor. Then, a laser pulse is focused onto the material layer where a bubble is induced and evolves into a jet that is propelled forward [9]. Once the jet reaches the acceptor, the material is deposited. If the material to transfer does not absorb the laser radiation an absorbing sacrificial layer is used. This layer coats the donor substrate so that it absorbs the laser radiation

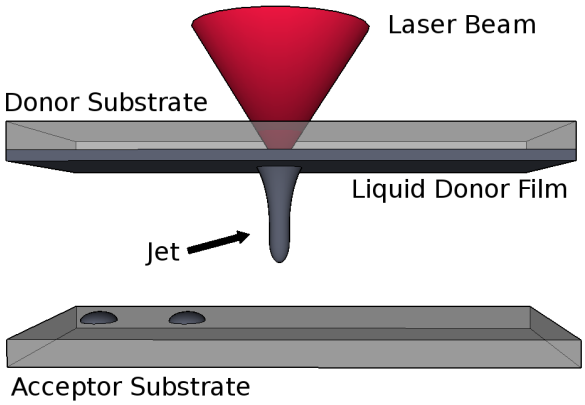

FIG. 1: Principle of operation of the LIFT technique.

[10]. Even though the scheme in Fig.1 indicates a downward transfer, liquids can also be transferred upwards if inverting the donor acceptor positions, since gravity does not play any role for such small jets [11].

LIFT has been widely studied through the systematic investigation of parameters such as laser fluence [12] or material viscosity [13]. Different laser pulse durations have been tested, though most of them in the short pulse regime: from a few nanoseconds to femtoseconds. However, longer pulses, of the order of hundreds of nanoseconds for example, have not been investigated yet. This regime is certainly interesting from both scientific and industrial points of view. On the one hand, the laser pulse interacts with the material during bubble expansion since the bubble expands in hundreds of nanoseconds. Thus, there is a fundamental interest because this kind of interaction has not been yet studied. On the other hand, many industrial lasers use laser pulses with durations of this order, thus reducing their cost. A detailed study and a feasibility test of the technique at this regime could help bringing LIFT to the industrial level reducing the costs

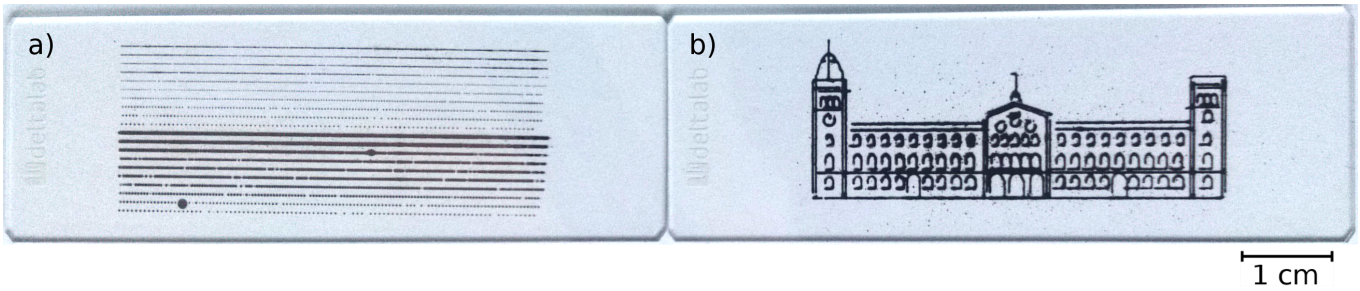

FIG. 2: Continuous lines (a) and University of Barcelona's logo (b) printed through LIFT.

of laser printing.

In this work LIFT in the hundred nanoseconds pulse regime is investigated by using an industrial marking laser. After proving the feasibility of the new pulse regime for printing, two different experiments were carried out to study LIFT in the long pulse duration conditions. The first one consisted on investigating the morphology of the deposited droplets, whereas the second one consisted on characterizing the dynamics of the transfer process by means of time-resolved imaging.

II. EXPERIMENTAL SETUP

Laser transfer was performed using a Nd:YAG (yttrium aluminium garnet) laser with a 1064 nm wavelength, a pulse width of approximately 120 ns and a beam waist of about 40 μm. Besides, since this is an industrial laser designed for engraving patterns it includes a set of two galvanometric mirrors that can scan the beam along the focal plane drawing preprogrammed patterns. A f-theta lens of 100 mm of focal length is placed at the exit of the laser. The laser was used in both pulsed and continuous wave (CW) mode depending on the experiment. The scanning speed could be varied at will.

The donor and acceptor substrates were $25{\times}75$ mm^2 microscope slides made out of glass. The chosen transfer material was a silver nanoparticle dispersion ink from Sigma Aldrich (ref.736481) because of its many possible applications for printing conductive patterns. Its particle size is smaller than 50 nm, the solid content is around 30–35 wt. % and the nominal viscosity of 8-10 $mPa{\cdot}s$. To produce the donor samples a 60 μL droplet of ink was deposited on a clean slide and spread using a blade coater, obtaining a film with a thickness of about 30 μm. Then, the donor was turned up-side-down and placed above the acceptor using coverslips of 200 μm as spacers. Finally the whole bunch was placed at the focal point of the laser. This process took approximately 5 min ensuring that the sample silver ink would not dry.

The time-resolved imaging setup, inserted into the previous setup, was used for the second experiment. Three different components were added: a light source, a CCD camera and a pulse generator. The light source consisted of a red LED connected to a pulse generator and two condenser lenses. The pulse generator synchronized the LED pulse (duration of about 100 ns) with the laser pulse at a controlled delay. Two lenses (25.4 and 35.0 mm of focal length), were aligned with the LED to condense light on a tiny spot, ensuring that most of light was used for imaging. A monochrome CCD camera from Diagnostic Instruments Inc. with an exposure time of 500 μs and coupled to a $20{\times}$ microscope objective with a numerical aperture of 0.42 were used. Both light source and camera setup were placed along the same optical axis in shadowgraphy configuration.

III. RESULTS AND DISCUSSION

The feasibility of LIFT for conductive inks printing with long pulses was proven through the systematic variation of the main process parameters (laser pulse energy and scan speed), showing that it was possible to print continuous lines (Fig.2a) and later complex patterns (Fig.2b). These were substantially larger than most patterns usually printed in previous works on LIFT [2], since an industrial-scale working laser instead of short-pulsed lasers focused through a microscope was used. Consequently, lines were wider. However, many industrial applications do not require microscopic resolution. For instance, mesoscopic realizations, like smart tags (RFID tags), do not require very high resolutions and present a clear industrial interest [14]. The optimization of the performance of LIFT with long pulses requires the study of the printing process.

A. Droplet Printing

In order to study the main features of droplet deposit the laser was scanned along the sample at a constant speed of 1000 m/s and a pulse rate of 1 kHz, conditions which allowed printing non-overlapping droplets. Different droplet arrays at different laser pulse energies were printed. By printing redundant arrays a greater number of droplets was obtained using the same donor substrate. This implied that any deviation that appeared in the

results due to inhomogeneities in the liquid donor film thickness could be diminished.

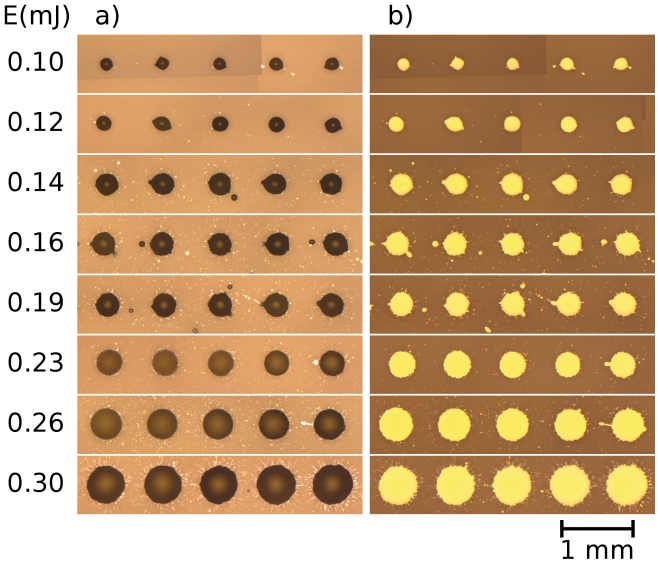

FIG. 3: Optical microscopy images of the droplets deposited at different laser pulse energies (indicated in each row): just after printing (a) and once they have been dried (b).

In Fig.3 droplets and their corresponding dried pixels from one of the experiments are shown. The laser pulse energy was varied from 0.01 to 0.30 mJ, and it can be observed how the first transferred droplets correspond to 0.1 mJ; thus, there is a minimum energy below which there is no transfer. It can be observed how as the laser pulse energy is increased the radius of the droplets also increases, from 80 μm at low energies (0.1 mJ) to 250 μm at the highest energy (0.3 mJ). These radii are substantially larger than those usually obtained with shorter donor pulses in which different parameters such as laser pulse energies of μJ were used [11, 15]. The droplets perimeter is rather uniform and well defined at low energies, whereas it has some splash at high energies and satellite droplets are found at intermediate energies. When comparing wet (a) and dry (b) droplets no apparent change in dimensions is observed.

Using confocal microscopy more information of the droplets could be obtained. Fig.4 shows profiles of selected pixels obtained with this technique. It can be observed how the radius clearly increases with energy too. However, thickness does not follow the same trend. Thickness is fairly constant around 0.5 μm till an energy of 0.16 mJ is reached, then it decreases. Also, as the radius increases the coffee-ring is much more visible. Coffee-rings appear in droplet solutions that contain particles in suspension as they are left to dry up [16]. After a LIFT event, the droplets, which contact line is pinned, start to dry. This changes the curvature of the droplet, which results in a Laplace pressure gradient and a capillary flow from the center toward the edges. Due to this flow, as droplets dry, nanoparticles tend to gather at the edges, leaving this characteristic ring and the M shape

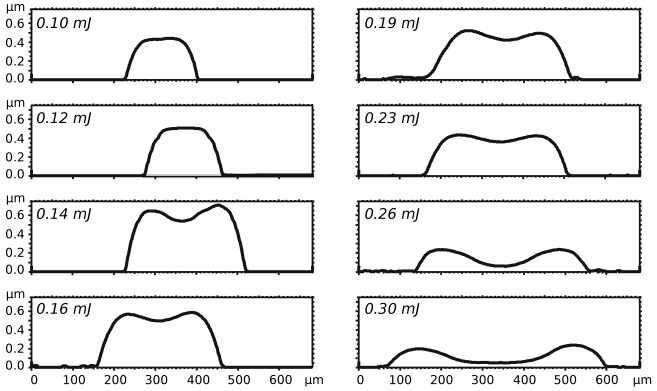

FIG. 4: Confocal microscopy profiles of dry pixels at different laser pulse energies.

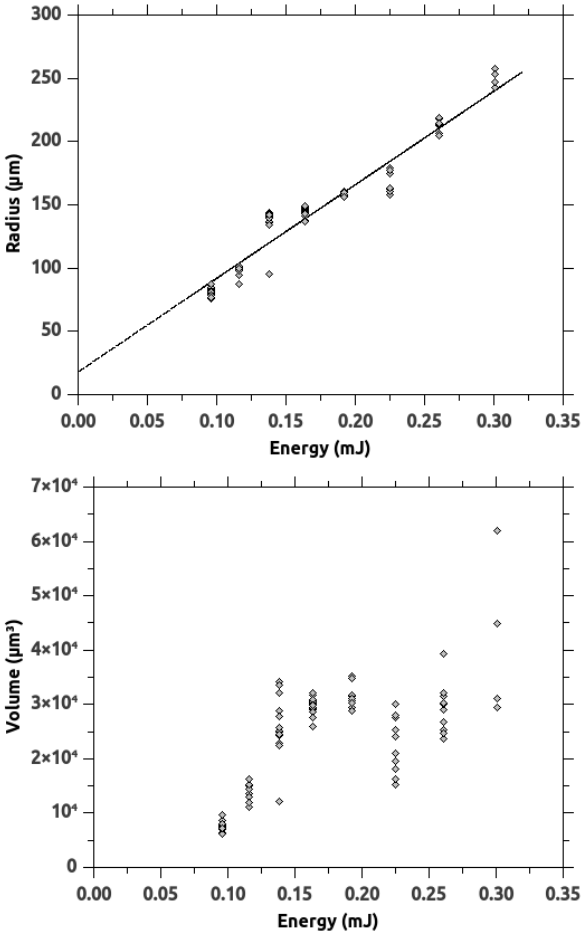

FIG. 5: Plots of the deposited pixel radius and volume versus laser pulse energy. The solid line corresponds to a linear fit.

observed in the pixel profiles.

A further study was carried out using optical microscopy images to obtain the pixel radius and confocal microscopy to get the respective volume. These data are plotted in Fig.5 as a function of laser pulse energy. The radius increases with energy in a clear linear trend. Similar results have been observed in other studies, however with considerably different conditions. For instance, N.T. Kattamis *et al.* used a sacrificial layer of polyimide, laser pulses of 15 ns and $\sim 10 \mu J$, and water with glycerol solutions [17]; and A. Patrascioiu *et al.* used femtosecond pulses with water and glycerol solutions also and a pulse energy of 2 μJ [11]. Though the parameters are different, laser pulse intensities for which there is LIFT in our experiment and the two mentioned ones are of the same order, around 50 MW/cm^2.

A rather different trend is observed in the volume data. Volume increases at low energies till it reaches a pulse energy of around 0.2 mJ. At this point, the volume seems to decrease and increase again. When comparing it to the radius data, it is noticeable how there is much more dispersion in volume than in radius.

Both radius and volume trends are substantially different from some previous LIFT studies where it was found that the volume-energy dependence was linear [4, 18, 19]. Those experiments were carried out with a few nanoseconds laser pulses and water/glycerol solutions. The main difference with the present experiment was pulse duration. In order to get more information about the transfer process, that could provide some insight on the reported differences, an imaging study of the transfer dynamics was carried out.

B. Liquid Ejection Dynamics

This experiment requires observing a really fast phenomenon that happens at the microsecond scale. For that, a 10^6 fps camera would be required, provided that image acquisition was carried out by means of fast photography. However, a different approach which does not involve the acquisition of very expensive devices is possible. If the phenomenon of study is repeatable enough a stroboscopic approach can be undertaken. It consists on taking several snapshots of the same event with different time delays respect to the beginning of the event. Later, by putting all the images together a stop-action movie of the phenomenon is obtained and the dynamics can be studied. This was the approach used in this section, according to the experimental setup in section II.

In order to obtain a snapshot of the transfer process the laser was activated and a single shot was produced. The laser pulse triggered the pulse generator which in turn triggered the LED and the camera. Thus, a picture with an exposure of 500 μs was taken. During that time the LED pulse, which length (about 100 ns) was much shorter than the camera exposure time and depended on the experiment, illuminated the sample at a very specific delay time respect the laser pulse. Therefore, the effective exposure time was determined by the LED pulse length. Using a computer-controlled xyz translation stage the sample was moved so that each LIFT process would take place in a different region of the slide and the uniformity of the donor was guaranteed for each event. Two energy studies were carried out, the first to observe the general fluid dynamics Fig.6a-c (LED pulse length of 100 ns), and the second considering a much challenging yet similar transfer as the used in the droplets printing experiment, Fig.7a-c (LED pulse length of 200 ns). Both experiments explored representative pulse energies of 0.1, 0.2 and 0.3 mJ.

Energy (mJ)	Front Velocity (m/s)	Bubble Radius (μm)	Weber Number
0.1	50	125	2.3×10^4
0.2	133	152	2.3×10^5
0.3	166	130	3.5×10^5

TABLE I: Obtained parameters of the time-resolved LIFT study of Fig.6a-c.

Time-resolved images of Fig.6a-c, correspond to a 1200 μm donor-acceptor gap distance so that the liquid ejection dynamics was clearly visible. Four different stages can be distinguished: bubble expansion, bubble burst, jet formation and deposition. Depending on the laser pulse energy some of the stages are more visible than others, however, they are present at all energy values. As the laser pulse is absorbed in the ink layer, a bubble is generated and because the inner pressure is very high, it expands until bursting. Comparing the three energy cases it is noted how as the energy is increased the burst is more powerful, starting earlier and lasting longer. A dimensionless number, the Weber number (ratio between kinetic and surface tension energies), is defined as

$$We = \frac{\rho v^2 l}{\sigma}, \tag{1}$$

where the considered length scale l is taken to be the bubble maximum radius, the characteristic velocity v is taken to be the front velocity, and the density ρ and the surface tension σ are ink parameters. It can be seen in Tab.I how large Weber numbers, above 10^4, are always found. This is consistent with the fact that the bubble expands in a turbulent manner, not being able to conserve the hemispherical shape, but bursting instead. The jet is formed when the bubble loses kinetic energy and surface tension becomes significant again. At the first moments of the jet formation, since the Weber number is still high, the jet is turbulent and not well outlined. When the jet finally contacts the acceptor substrate the deposition starts. At this final stage the jet becomes steadier till it forms a vertical straight line. Finally, the bubble deflates and the jet is broken in small little droplets. It is also observed that the deposition stage is maximum at a pulse energy of 0.2 mJ, as seen in Fig.6b.

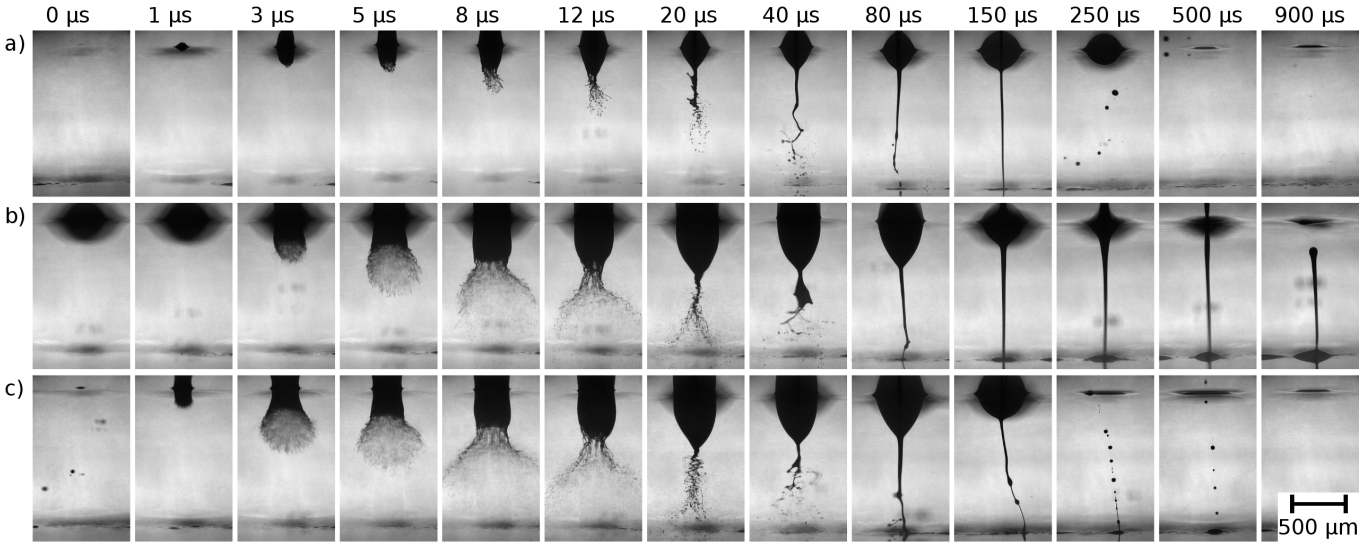

FIG. 6: Series of time-resolved images of a laser-induced forward transfer. Pictures on the same row correspond to the same pulse energy, 0.1 mJ (a), 0.2 mJ (b) and 0.3 mJ (c). Donor acceptor gap is 1200 μm. The donor film is located in the top of the images, the acceptor substrate in the bottom and the laser beam impinges from above.

The transfer process has been analysed in other studies, however, the *burst* stage is rarely present, and when it is observed it seldom turns into a jet. M. Duocastella *et al.* carried a time-resolved energy study of LIFT using a titanium sacrificial layer and a glycerol-water 50% (v/v) solution [15]. They observed how at low energies ($\sim 34 \mu J$) the kinetic energies were not high enough and even though a jet was created, it retracted not being able to touch the acceptor substrate. At intermediate energies a clear bubble was formed and expanded leading to a well defined straight jet. At high energies ($\gtrsim 0.3\ mJ$) the bubble bursted and no jet was formed. So, unlike our experiment, at bubble burst conditions no droplet was transferred and only a splash was visible on the acceptor. Otherwise, Boutopoulos *et al.* using a silver nanoparticle ink with and without sacrificial layer observed a much more similar burst-jet behaviour [20]. When using high energies and a titanium sacrificial layer the burst occurs and turns into a turbulent jet. On the other hand, when no sacrificial layer is present the burst takes place at lower energies and it is much more aggressive with a more erratic jet shape. The differences found between the present case and the previous studies, all of them corresponding to much shorter laser pulses, indicate that indeed for relatively long laser pulses (hundreds of ns) a substantially different dynamics sets on, which could also account for the differences encountered in the deposits.

A more challenging situation was considered when decreasing the donor-acceptor gap distance to 250 μm, Fig.7a-c. This situation is much closer to the droplet printing conditions of the previous section and, since the donor is closer to the acceptor, the dynamics changes. By looking at the image of Fig.6a-c and supposing a 250 μm gap it is clear that LIFT will take place in the jet regime for low energies Fig.6a and in the bubble-contact regime at high energies Fig.6c [21]. In all the images corresponding to the droplet printing experiment situation the contrast was corrected because the sample was poorly illuminated due to the narrower gap.

Indeed, as previously suggested, at the highest energy (0.3 mJ) transfer takes place in a bubble-contact basis, whereas a jet is well defined at the lowest energy (0.1 mJ). The four stages that took part in transfer in the previous experiment are not always present now because of the acceptor proximity. At the lowest energy, Fig.7a, bubble expansion, burst expansion, jet formation and deposition are visible and distinguishable. As the energy is increased, Fig.7b, the bubble expansion is faster and the burst is more visible. Unlike before, the burst contacts the surface and the deposition of material starts. A jet is formed afterwards but it is not the instigator of the deposit. At the highest energy, Fig.7c, the bubble expansion is so fast that it explodes just on the acceptor substrate. Then it recoils and ends up forming a very small jet as the bubble collapses. In this case, the burst and jet stages are not really as complete as before. Comparing the deposition time of the three energies, it can be observed how at 0.2 mJ the deposition is approximately 40 μs longer. This is in agreement with the previous time-resolved experiment, in which the deposit time was found to be also longer at intermediate energies of 0.2 mJ. However, if the total time scale of both experiments is compared, it is clear that for a larger gap distance the deposit time is longer. Moreover, the transfer mechanism changes from a jet deposit to a bubble-contact deposit.

So, observing this behaviour two transfer effects can be pointed out. The first, for large donor-acceptor gaps, as energy increases the bubble burst starts sooner and is

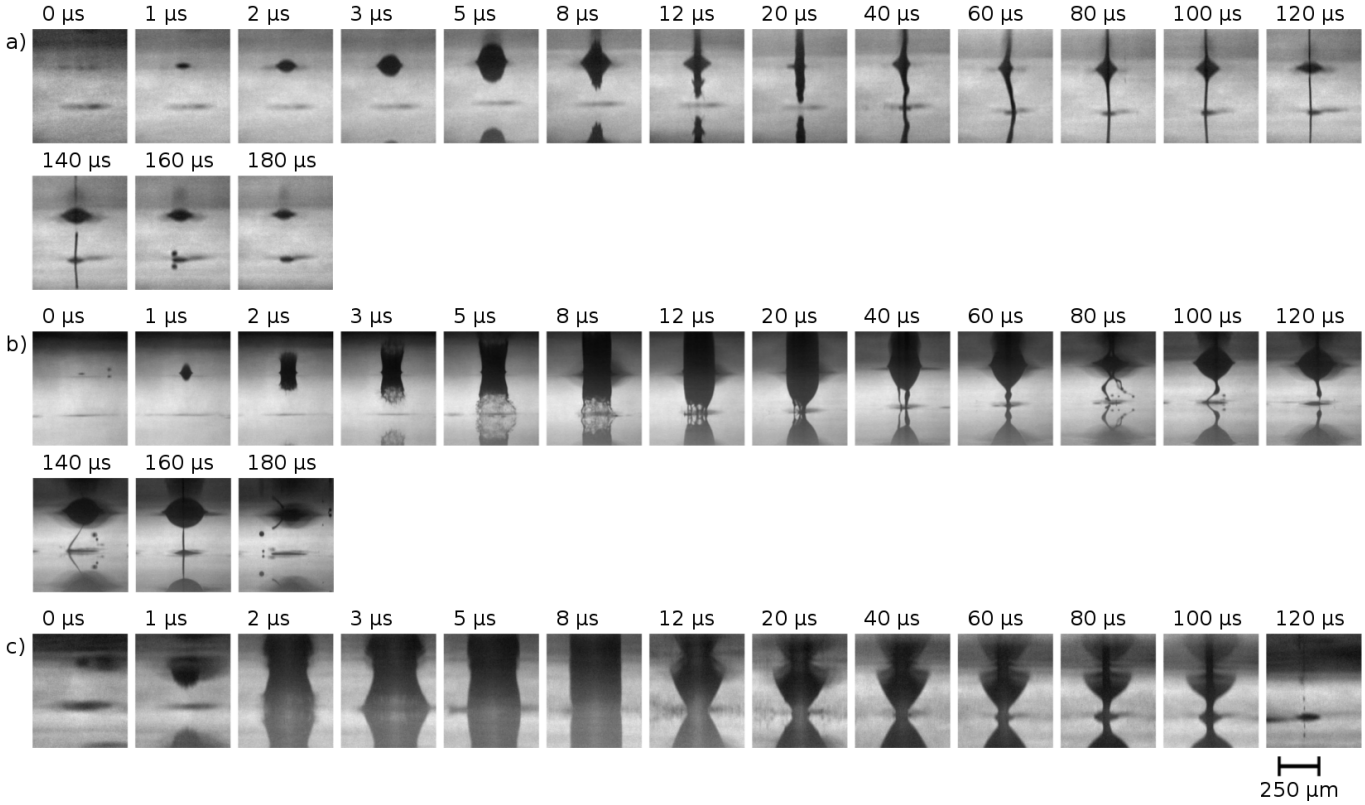

FIG. 7: Series of time-resolved images of a laser-induced forward transfer. Pictures on the same row correspond to the same pulse energy, 0.1 mJ (a), 0.2 mJ (b) and 0.3 mJ (c). Donor acceptor gap is 250 μm. The donor film is located in the top of the images, the acceptor substrate in the bottom and the laser beam impinges from above.

more violent; however, it always retracts and forms a jet. The second, for small donor-acceptor gaps, the stages of transfer change as the energy is increased, the material transfer evolves from being a jet deposit to a bubble-contact deposit. Thus, two different transfer regimes are found as a function of laser pulse energy.

In section III A a possible transfer behaviour change was proposed when discussing volume-energy data, Fig.5, around a laser pulse energy of 0.2 mJ. Therefore, some correlation between the liquid ejection dynamics and the deposited droplets is apparent, since time-resolved images from Fig.6a-c also indicate that a change in the trend takes place above 0.2 mJ. In the pixel profiles it is also observed how above 0.2 mJ the morphology of the pixels changes, becoming thinner. Nevertheless, this change in transfer behaviour is not reflected on the droplet radius as a function of the energy, which always follows a linear trend.

Duocastella *et al.* observed how when the bubble is generated, a plasma is induced in the donor-ink interface at the very first instants of the laser pulse, lasting approximately 80 ns for a 5 ns laser pulse [15]. In the present case a plasma might be formed as well by the longer laser pulse. Plasmas are characterized by their critical density, below which the plasma partially transmits and reflects electromagnetic radiation (1064 nm laser radiation in this case) and above which it becomes a perfect reflector, shielding absorption [22]. It can be assumed that at low laser pulse energies the critical density is not attained yet, but it may be reached at higher energies. As the laser pulse energy increases, the delivered energy is higher and the transfer process should last longer, as observed from 0.1 to 0.2 mJ. So, at 0.3 mJ an even longer deposit time would be expected. Nonetheless, that is not observed in neither time-resolved images at 1200 μm nor 250 μm gaps. It would be plausible, therefore, that the plasma critical density would be achieved around 0.3 mJ before the end of the laser pulse. Thus, for an energy of 0.3 mJ at the start of the laser pulse a plasma would be generated and the laser pulse would keep on heating that plasma till it reached the critical density, at which point the rest of the laser pulse would be reflected. Thus, even though the pulse energy is higher than before it would not be totally delivered to the ink, which could account why the deposit time is less and why the volume of the droplets shows and apparent decrease above 0.2 mJ. This plasma shielding effect proposed to account for the evolution observed in both deposit time and droplet volume does not seem to influence the bubble burst, which is more violent as the laser pulse energy

increases. It is reasonable to think that the bubble expansion speed depends mainly on the instantaneous laser intensity (rate of change of instantaneous fluence). For increasing laser pulse energies, the instantaneous power per unit area increases too, causing the bubble speed to be greater and the bubble burst more aggressive. Less liquid is displaced but at a higher speed.

Depending on the laser pulse energy the deposition mechanism seems to change, from jet-contact to bubble-contact as remarked in Fig.7a-c. This two-regime behaviour correlates pretty well with the volume-energy evolution. However, it is not observed in the radius plot. At the lowest energy (0.1 mJ), Fig.7a, the deposit takes place through jet contact. The material is slowly transferred and the radius of the deposited droplet will mostly depend on the amount of transferred material. As the energy is increased to 0.2 mJ, Fig.7b, the transfer mechanism is not so clear, showing the transition from jet to bubble-contact. Nevertheless, the deposit time is increased, which accounts for the increase in droplet volume and radius. As the energy further increases, however, the deposit time is less, Fig.7c, as already discussed. One would expect, then, the radius of the droplets to decrease too, but that is not observed in Fig.5a which shows a monotonous increase. This can be attributed to the bubble-contact mechanism. As the energy increases the bubble burst is more violent and the acceptor surface is covered by the burst during contact. It can be assumed, therefore, that the droplet radius will be determined by the area wetted by the bubble contact (through contact line pinning) rather than by the transferred column of liquid, and this would finally account for the increase observed in the radius evolution. In both regimes, jet and bubble-contact, the radius increases with the energy even though the transfer dynamics is different. Nevertheless, a considerably more complex study should be carried out in order to determine the origin of the linear trend of the radius-energy data with no discontinuity.

C. Feasibility test

One of the advantages of using LIFT over other more conventional printing techniques is the capacity of using the same laser for other treatments like ablation or sintering in addition to printing. Usually, inkjet-printed electrical circuits are placed in an oven where they are sintered in order to achieve the desired conductive properties. Though effective, this process might damage other sensible parts of the circuit, thus a local sintering technique would be convenient. LIFT and laser sintering fulfil this requirement and allow local material treatment.

In order to prove the viability of the technique to produce functional electrical circuits, a series of silver ink paths were printed, Fig.8. Using the laser in a pulsed mode at 1 kHz, in order to obtain lines, droplets were printed with some overlap between them [23]. Setting the scanning speed at 100 mm/s and the laser pulse energy to 0.12 mJ an overlap of the 20 % was reached, optimum for

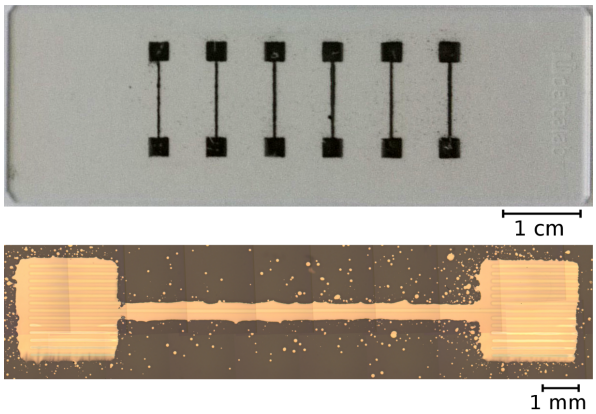

FIG. 8: Optical image of silver nanoparticle paths deposited using LIFT (top). Microscopy image of one of the paths (bottom).

the generation of the lines presented in Fig.8, with wider ends to act as contacts. In order to sinter the paths, the laser was scanned along the path in CW mode at a velocity of 6 mm/s and a power of 750 mW. In the bottom image of Fig.8 a more detailed path is shown. Straight horizontal lines corresponding to the laser sintered area can be slightly appreciated on the path. Measured resistivity values before sintering were 54000 $\mu\Omega \cdot cm$; after sintering the resistivity was reduced to 22 $\mu\Omega \cdot cm$. The nominal resistivity of the oven sintered ink is $\sim$2 $\mu\Omega \cdot cm$, thus the sintering process did not reach the total coalescence of the nanoparticles, but the resistivity decreased three orders of magnitude, so the sintering process was effective.

IV. CONCLUSIONS

The feasibility of laser-induced forward transfer was proven using an industrial laser with long laser pulses by transferring an absorbing conductive ink of silver nanoparticles.

When performing an energy study it was observed that both wet and dry droplets (pixels) increase their radius linearly with the pulse energy. However, a non monotonous trend was found for the volume evolution. This change was also observed in the pixels morphology.

The time-resolved study of the transfer dynamics revealed that, independently of the pulse energy, the transfer takes place in four steps: bubble expansion, bubble burst, jet formation and deposition. As energy increases the deposit time increases, reaching a maximum around 0.2 mJ, above which it decreases. This change in deposit time correlates well with volume-energy data and could be attributed to the onset of the critical electron density of the plasma created within the liquid film. At low energy regime ($\lesssim$0.2 mJ) the laser pulse would not be energetic enough to reach the critical density, so as the laser pulse energy increased more energy would be transmitted

to the liquid and the deposit would be longer. Otherwise, in the high energy regime ($\gtrsim 0.2\ mJ$) the critical density would be reached, so part of the laser pulse would be reflected, shortening the deposit time.

The time-resolved imaging study in deposit conditions (250 μm gap) reveals that the four transfer stages are not always present. For low energies all of the stages are present, whereas for high energies the bubble burst is so powerful that it reaches the acceptor substrate before collapse and deposit starts. At low energies the transfer process is mediated by jet formation whereas at high energies it corresponds to a bubble-contact transfer.

By means of printing lines through droplets overlap, conductive paths can be successfully printed. A further laser sintering treatment proved their functionality as interconnects, decreasing the resistivity three orders of magnitude down to 20 $\mu\Omega \cdot cm$, an acceptable value in many applications.

ACKNOWLEDGMENTS

The advisory work of Dr. P.Serra is greatly acknowledged, as well as the assistance of Dr. J.M.Ferrnández-Pradas in the laboratory. Many thanks as well to my laboratory colleagues C. Froilán and F. Caballero, and my family and friends.

[1] Calvert P., 2001. Inkjet Printing for Materials and Devices. *Chemistry of Materials*, **13** (10), 3299-3305.

[2] Arnold C.B., Serra P., Piqué A., 2007. Laser Direct-Write Techniques for Printing of Complex Materials. *MRS Bulletin*, **32**, 23-31.

[3] Piqué A., Kim H., 2014. Laser-Induced Forward Transfer of Functional Materials: Advances and Future Directions. *Journal of Laser Micro/Nanoengineering*, **9** (3), 192-197.

[4] Duocastella M., Fernández-Pradas J.M., Domínguez J., Serra P., Morenza J.L., 2008. Printing biological solutions through laser-induced forward transfer. *Applied Physics A*, **93**, 941-945.

[5] Hennig G. *et al.*, 2012. Lasersonic® LIFT Process for Large Area Digital Printing. *Journal of Laser Micro/Nanoengineering*, **7** (3), 299-305.

[6] Makrygianni M., Kalpyris I., Boutopoulos C., Zergioti I., 2014. Laser induced forward transfer of Ag nanoparticles ink deposition and characterization. *Applied Surface Science*, **297**, 40-44.

[7] Rapp L., Constantinescu C., Delaporte P., Alloncle A.P., 2014. Laser-induced forward transfer of polythiophene-based derivatives for fully polymeric thin film transistors. *Organic electronics*, **15**, 1868-1875.

[8] Serra P., Colina, M., Fernández-Pradas J.M., 2004. Preparation of functional DNA microarrays through laser-induced forward transfer. *Applied Physics Letters*, **85** (9), 1639-1641.

[9] Duocastella M., Fernández-Pradas J.M., Serra P., Morenza J.L., 2008. Jet formation in the laser forward transfer of liquids. *Applied Physics A*, **93**, 453-456.

[10] W.A. Tolbert W.A., Lee I.-Y.S., Doxtader M.M., Ellis E.W., Dlott D.D., 1993. High-speed color imaging by laser-ablation transfer with dynamic release layer - Fundamental Mechanism. *Journal of Imaging Science and Technology*, **37** (4), 411-422.

[11] Patrascioiu A., Duocastella M., Fernández-Pradas J.M., J.L. Morenza J.L., Serra P., 2011. Liquids microprinting through a novel film-free femtosecond laser based technique. *Applied Surface Science*, **257**, 5190-5194.

[12] Yan J., Huang Y., Xu C., Chrisey D.B., 2012. Effects of fluid properties and laser fluence on jet formation during laser direct writing of glycerol solution. *Journal of Applied Physics*, **112**, 083105.

[13] Mathews S.A., Auyeung R.C.Y., Kim H., Charipar N.A., and Piqué A., 2013. High-speed video study of laser-induced forward transfer of silver nano-suspensions. *Journal of Applied Physics*, **114**, 064910.

[14] Yang C.C., Tsai H.Y., Yang C.C., Hsiao W.T., Huang K.C., 2014. Fabricating planar spiral inductances for a wireless charging module by using 355 nm ultraviolet laser ablation. *Applied Physics A*, **117**, 69-75.

[15] Duocastella M., Fernández-Pradas J.M., Morenza J.L., Serra P., 2009. Time-resolved imaging of the laser forward transfer of liquids. *Journal of Applied Physics*, **106**, 084907.

[16] Deegan R.D., Bakajin O., Dupont T.F., Huber G., Nagel S.R., Witten T.A., 1997. Capillary flow as the cause of ring stains from dried liquid drops. *Nature*, **389**, 827-829.

[17] Kattamis N.T., Purnick P.E., Weiss R., Arnold C.B., 2007. Thick film laser induced forward transfer for deposition of thermally and mechanically sensitive materials. *Applied Physics Letters*, **91**, 171120.

[18] Duocastella M., Patrascioiu A., Fernández-Pradas J.M., Morenza J.L., Serra P., 2012. On the correlation between droplet volume and irradiation conditions in the laser forward transfer of liquids. *Applied Physics A*, **109**, 5-14.

[19] Colina M., Duocastella M., Fernández-Pradas J.M., Serra, P., Morenza J.L., 2006. Laser-induced forward transfer of liquids: Study of the droplet ejection process. *Journal of Applied Physics*, **99**, 084909.

[20] Boutopoulos C., Kalpyris I., Serpetzoglou E., Zergioti I., 2014. Laser-induced forward transfer of silver nanoparticle ink: time-resolved imaging of the jetting dynamics and correlation with the printing quality. *Microfluid Nanofluid*, **16**, 493-500.

[21] Duocastella M., Kim H., Serra P., Piqué A., 2012. Optimization of laser printing of nanoparticle suspensions for microelectronic applications. *Applied Physics A*, **106**, 471-478.

[22] Mulser P., Bauer D., 2010. The Laser Plasma: Basic Phenomena and Laws. In: Springer, *High Power Laser-Matter Interaction*. Berlin: Springer-Verlag Berlin Heidelberg, 5-89.

[23] C. Florian C., Caballero-Lucas F., Fernández-Pradas J.M., Artigas R., Ogier S., Karnakis D., Serra P., 2015. Conductive silver ink printing through the laser-induced forward transfer technique. *Applied Surface Science*, **336**, 304-308.